CHEMISTRY
A EUROPEAN JOURNAL

DOI: 10.1002/chem.200800877

The Role of Noninnocent Solvent Molecules in Organocatalyzed Asymmetric Michael Addition Reactions

Mahendra P. Patil and Raghavan B. Sunoj*[a]

Abstract: A proline-catalyzed asymmetric Michael addition between ketones and *trans*-β-nitrostyrene was studied by using the density-functional theory with mPW1PW91 and B3LYP functionals. Improved insight into the enantio- and diastereoselective formation of γ-nitroketones/-aldehydes is obtained through transition-state analysis. Consideration of the activation parameters obtained from gas-phase calculations and continuum solvation models failed to reproduce the reported experimental stereoselectivities for the reaction between cyclohexanone and 3-pentanone with *trans*-β-nitrostyrene. The correct diastereo- and enantioselectivites were obtained only upon explicit inclusion of solvent molecules in the diastereomeric transition states that pertain to the C–C bond formation. Among the several transition-state models that were examined, the one that exhibits cooperative hydrogen-bonding interactions with two molecules of methanol could explain the correct stereochemical outcome of the Michael reaction. The change in differential stabilization that arises as a result of electrostatic and hydrogen-bonding interactions in the key transition states is identified as the contributing factor toward obtaining the correct diastereomer. This study establishes the importance of including explicit solvent molecules in situations in which the gas-phase and continuum models are inadequate in obtaining meaningful insight regarding experimental stereoselectivities.

Keywords: density functional calculations · Michael addition · organocatalysis · solvent effects · stereoselectivity · transition states

Introduction

Organocatalysis by using small molecules has generated considerable interest as a viable tool for asymmetric synthesis over the last half a decade.[1] Among several organocatalysts developed for asymmetric reactions, proline and its analogues possess special importance owing to their ability to serve as catalysts for several C–C bond-forming reactions.[2] The catalytic ability of L-proline was successfully exploited in a range of quintessential reactions, such as the Mannich,[3] Michael,[4] Robinson annulation,[5] α-amination,[6] α-oxidation,[7] and α-alkylation reactions.[8] Mechanistic studies in conjunction with synthetic developments have contributed immensely to the rapid success of organocatalytic reactions.[9,10] Careful examination of the available literature conveys that the mechanistic course of the proline-catalyzed aldol reaction is one of the most widely reported among the organocatalytic reactions, whereas the underlying mechanistic information on the proline-catalyzed Michael reaction is rather limited.

The nucleophilic addition of enolates to an electrophilic multiple bond, popularly known as the Michael reaction, offers a convenient route toward the synthesis of remote functionalized targets.[11] Among the large number of electrophiles, nitroolefins are extensively employed as substrates in stereoselective Michael addition reactions.[12] Pioneering applications of the proline-catalyzed Michael addition between ketones and *trans*-β-nitrostyrene (nitrostyrene hereafter) have been demonstrated by List et al.[4b] and Enders and Seki.[4d] Several modifications of proline have been effectively employed in asymmetric reactions.[13,14] In a series of related developments, an impressive array of catalysts, such as chiral pyrrolidine–pyridine,[15] pyrrolidine sulfonamide,[16] 3,3′-bimorpholine derivatives,[17] *trans*-4-hydroxyprolylamide,[18] chiral amine—thiourea,[19] and diphenylprolinol silyl ethers,[20] have been successful in the Michael addition of aldehydes (or ketones) to nitroolefins. Very recently, pro-

[a] M. P. Patil, Prof. Dr. R. B. Sunoj
Department of Chemistry
Indian Institute of Technology Bombay
Powai, Mumbai 400076 (India)
Fax: (+91)22-2572-3480
Fax: (+91)22-2576-7152
E-mail: sunoj@chem.iitb.ac.in

Supporting information for this article is available on the WWW under http://dx.doi.org/10.1002/chem.200800877.

linal dithioacetal and 4,4′-disubstituted L-proline were identified as efficient organocatalysts for the addition of an aldehyde to nitrostyrene with excellent enantioselectivities.[21]

Although the quest for new catalysts for Michael reactions continues to grow, parallel attempts toward gaining mechanistic insight are relatively less available.[22] The generally accepted catalytic cycle for proline-catalyzed reactions of a ketone or aldehyde with an electrophile is depicted in Scheme 1. The proline-catalyzed reaction mainly involves

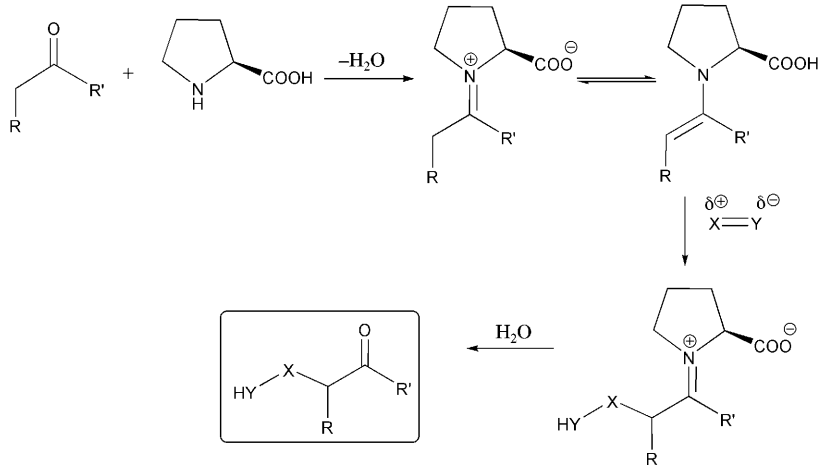

Scheme 1. Key steps involved in a proline-catalyzed Michael addition between a ketone and an electrophile (X=Y).

three key steps: the formation of an enamine, the addition of the enamine to the electrophile, and the subsequent hydrolysis to expel the catalyst from the product. The energetics associated with the formation of an enamine between acetone and proline is investigated elsewhere.[23] In general, it is assumed that the enamine formation is faster compared with the ensuing nucleophilic addition of the enamine to the electrophile.[24] Further, the hydrolysis step that leads to the expulsion of the catalyst is also reported to involve only a low energy barrier.[9c,25] On the basis of the available reports on enamine organocatalysis, it is now accepted that the stereoselectivity in enamine-catalyzed C–C bond-forming reactions is critically dependent on the addition of an enamine to the electrophile.

According to the model developed by Houk and co-workers, the transition state for the addition of the proline enamine to an electrophile involves intramolecular hydrogen bonding between the carboxylic acid group and the developing alkoxide ion (in which the enamine adds to a carbonyl group).[9,10] The differential stabilization of the transition states in stereochemically different modes of approaches (addition at the *re* and *si* faces) between the enamine and the electrophile is the primary factor responsible for the observed selectivity in these reactions.[26] The importance of hydrogen bonding offered by the catalyst has been reported in a variety of reactions.[9,27] Recent computational studies on organocatalyzed Michael addition reactions also support this transition-state model, which permits intramolecular hydrogen bonding.[22] In general, the agreement between the predicted stereoselectivities in organocatalyzed reactions, by using the transition-state model proposed by Houk et al., is quite good.[10b,28] As transition states for such reactions are polarized, the effect of solvation is incorporated through the continuum solvation models in most of these studies. However, a systematic attempt to evaluate the role of explicitly included solvent molecules on the reaction energetics is conspicuously absent. The inclusion of explicit solvents in transition states has been useful in bringing out salient mechanistic features associated with a range of interesting reactions.[29]

Transition-state studies that incorporate explicit solvents assume additional significance in the context of organocatalyzed Michael addition reactions. It is particularly noteworthy that the reaction rate and stereoselectivities of the organocatalyzed Michael addition of ketones to nitrostyrene has been improved in polar protic solvents, such as methanol or isopropanol, relative to that obtained in dimethyl sulfoxide (DMSO) as the solvent.[30] These experimental evidences allude to a more direct participation of the solvent molecules, apart from serving as a polar continuum medium, toward deciding the mechanistic course and the observed selectivities in such reactions. Herein, we have undertaken a comprehensive investigation that uses density functional theory (DFT) methods to understand the factors that control the stereoselectivity in proline-catalyzed Michael reactions between a range of ketones and nitrostyrene. This study further thrives to establish the importance and the role of solvent molecules in stereoselective Michael reactions. The results obtained by considering various solvent-assisted transition-state stabilizations for the Michael addition reaction are illustrated in the following sections.

Results and Discussion

A proline-catalyzed Michael addition between ketones/aldehydes with nitrostyrene is investigated herein (Scheme 2). The enamines derived from proline and carbonyl compounds such as propanal (**1**), 3-pentanone (**2**), and cyclohexanone (**3**) offer prochiral faces towards the addition to β-nitrostyrene. Such addition reactions can, therefore, result in four stereoisomeric products (two pairs of enantiomers). Additionally, the *syn* and *anti* orientations of the enamine double bond, with respect to the carboxylic acid group of

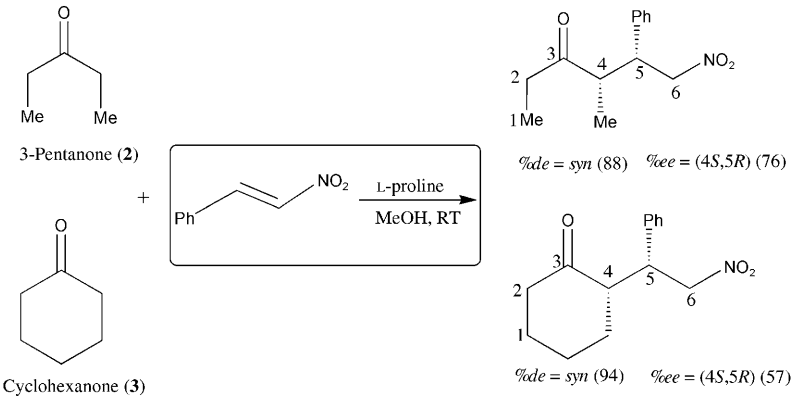

Scheme 2. Experimental stereoselectivities for the proline-catalyzed Michael addition of **2** and **3** with nitrostyrene.

the pyrrolidine ring would lead to a total of eight important modes of approaches between the enamine and nitrostyrene. Four key modes of addition between nitrostyrene and *syn* or *anti* enamines through their prochiral faces (*re*/*si*) are depicted in Scheme 3.

In general, the transition states for these modes of approaches, *a-si*, *a-re*, *s-si*, and *s-re* are stabilized by hydrogen-bonding interactions between the carboxylic group of the enamine and the nitro group of nitrostyrene (see below). The transition states are successfully located at the mPW1PW91/6–31G* and B3LYP/6–31G* levels of theory.[31] It is identified that the four transition states depicted in Scheme 3 have lower energy than other possibilities.[32]

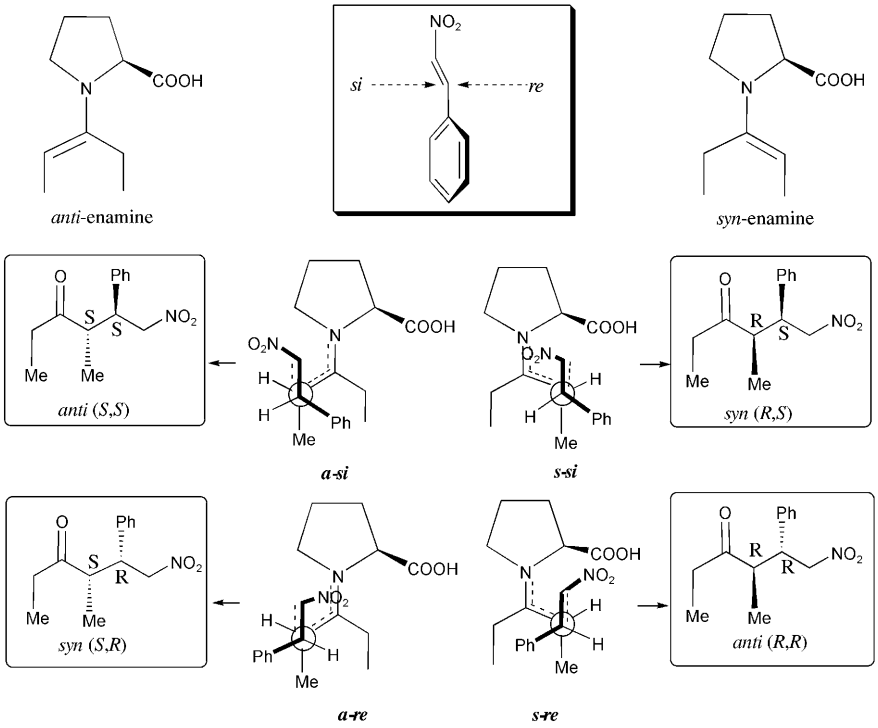

Scheme 3. Important stereochemical modes of addition of an enamine derived from proline and **2** with nitrostyrene.

These four lower-energy diastereomeric transition states are, therefore, considered toward estimating the stereoselectivity in the Michael reaction.

The discussion is organized into two major sections. First, the addition between the proline enamine and nitrostyrene is considered without the inclusion of any explicit solvent molecules in the transition state. Second, discussions on the role of explicitly included solvent molecules on the energetics and stereoselectivity are provided. We aim to propose improved transition-state models for Michael addition reactions in which the commonly employed models fail to reproduce the correct stereochemical outcome of the reaction. The primary motivation for considering explicit solvent molecules is progressively delineated such that the eventual discussion focuses on the newly proposed transition-state model for the Michael addition between proline enamines and β-nitrostyrene.

Unassisted pathway: The transition states for the addition of *anti* and *syn* enamines to the *si* and *re* faces of nitrostyrene were first located in the gas phase. These transition states are labeled *a-si*, *a-re*, *s-si*, and *s-re* (Scheme 3). The optimized geometries of the transition states for a representative case (3-pentanone enamine) are provided in Figure 1. The noticeable charge separation in the transition state is expected upon addition of the enamine to nitrostyrene.[33] To obtain improved estimates of the reaction energetics, continuum solvent effects are incorporated by computing the single-point energies by using the polarizable continuum model with methanol as the dielectric continuum at the mPW1PW91/6–311G** level (*M1*) on the gas-phase geometries obtained at the mPW1PW91/6–31G* level of theory. The same series of calculations are also performed by using the B3LYP functional (*M2*).

It is well established that various weak interactions play a critical role in proline-catalyzed aldol reactions toward providing the all important differential stabilization between the

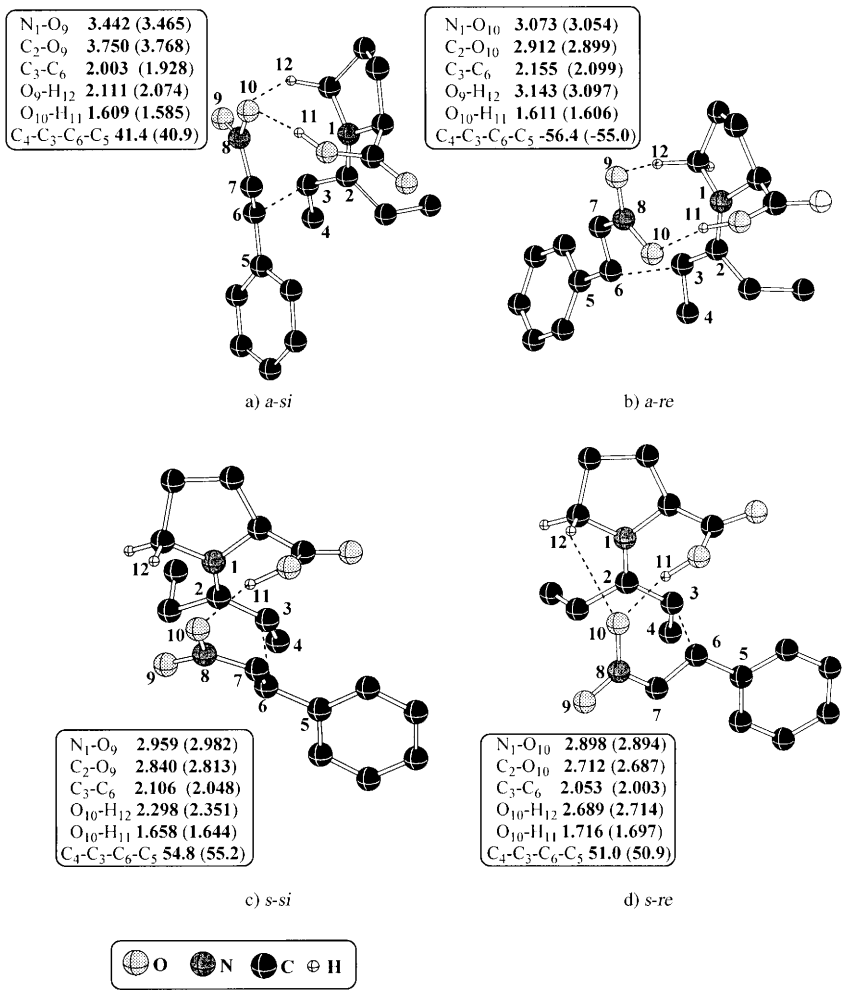

Figure 1. The mPW1PW91/6–31G* optimized transition-state geometries of four stereochemical modes of addition for enamines (derived from proline and **2**) to nitrostyrene. The values in parentheses refer to the geometric parameters at the B3LYP/6–31G* level of theory. Only selected hydrogen atoms are shown for clarity. Angles are given in degrees and distances in Å.

most favored and other diastereomeric transition states.[10b,34] These interactions include 1) the hydrogen bonding between the developing alkoxide species with the hydrogen atom of the carboxylic group and the methylene hydrogen atom adjacent to the nitrogen atom of the pyrrolidine ring and 2) Coulombic interactions between the incipient iminium and alkoxide moieties. The geometric distortion around the iminium/enamine part of the transition state has also been reported to influence to the activation barrier.[10b,34] It has also been noticed that the iminium moiety maintains a more planar geometry for cases in which the predicted activation barrier is low. The optimized geometries of the transition states for the Michael addition of **2** to nitrostyrene, as shown in compounds **1a–d**, clearly indicate a number of short interatomic contacts (Figure 1). For instance, the $O_{10}\cdots H_{11}$ distance exhibits a short hydrogen-bonding interaction between the carboxylic acid proton and the developing nitroxide ion. Stabilizing interactions of these kinds are further examined by evaluating topological features, such as electron density, at the bond critical points between the interacting atoms within the "atoms-in-molecule" framework. In the most preferred mode of addition, according to the computed free energies of activation in the condensed phase, an additional CH···π interaction is identified (i.e., **1a**, Figure 1).[35] Careful analysis of the degree of stabilization of the transition states achieved through the above-mentioned interactions reveals subtle changes in the net interaction, depending on the stereochemical mode of addition.[36]

To examine the effect of basis sets on computed geometries of the transition states, the four diastereomeric transition states given in Figure 1 were re-optimized at the mPW1PW91 level of theory using different basis sets (see the computational details and Tables S1–S4 in the Supporting Information for more details). The changes in the structural parameters are very minimal; further, the reaction coordinates are nearly the same, though the inclusion of a polarization function on the hydrogen atoms resulted in slightly shorter hydrogen-bonding contacts. A comprehensive analysis of the transition-state geometries obtained at the mPW1PW91 level across different basis sets is provided in the Supporting Information.

In the case of **3**, the nature and type of interactions are very similar to **2**. The key geometric features of the transition states for the addition of **3** to nitrostyrene are provided in Figure 2. In the *a-re* mode of addition, the developing nitroxide ion enjoys a relatively more effective hydrogen-bonding network ($O_9\cdots H_{12}$ and $O_{10}\cdots H_{11}$).

The computed activation barriers for different substrates in the gas and solvent phases are provided in Table 1. The free energies of activation were lowered upon including the bulk solvation effects relative to the gas phase, thus indicating that the transition states enjoy additional stabilization in a polar continuum such as methanol.[30] It is further noted that the relative trends in the activation barriers exhibit slight variations than that found by using the gas-phase barriers for diastereoisomeric transition states. The diastereo- and enantioselectivities were calculated using the relative energies of four transition states (Figures 1 and 2) on the basis of the absolute rate theory.[10b,34] The diastereomeric

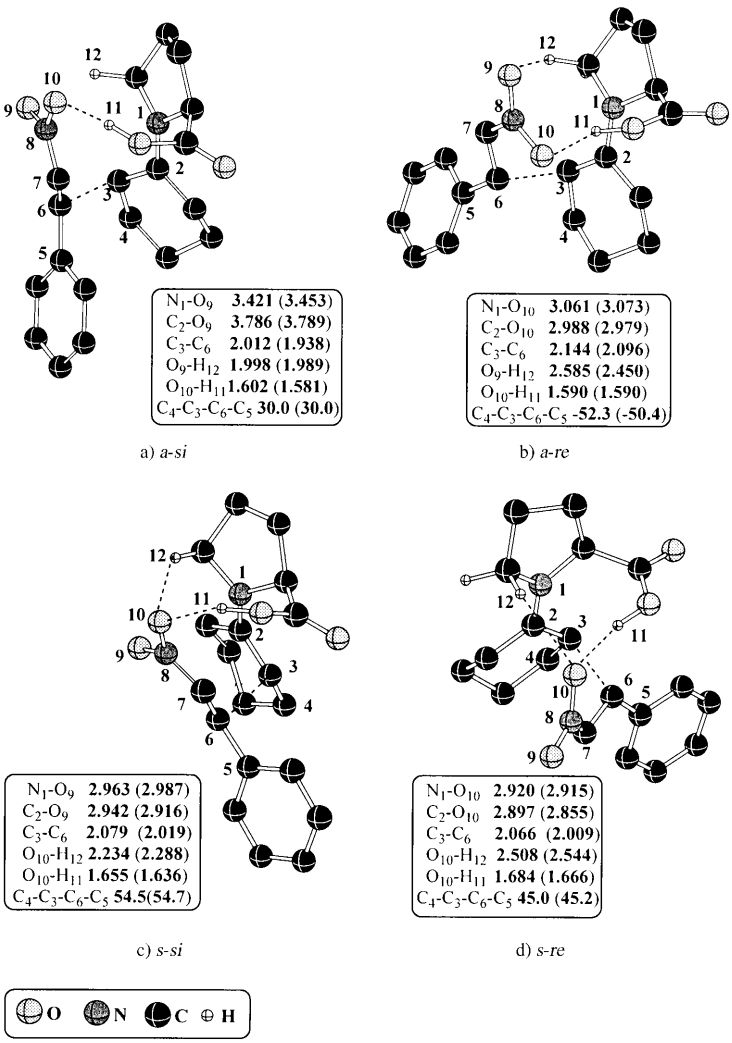

Figure 2. The mPW1PW91/6–31G* optimized transition-state geometries of four stereochemical modes of addition for enamines (derived from proline and **3**) to nitrostyrene. The values in parentheses refer to the geometric parameters at the B3LYP/6–31G* level of theory. Only selected hydrogen atoms are shown for clarity. Angles are given in degrees and distances in Å.

excess was computed by considering the difference between the activation barriers of the most energetically favored transition state and the transition state that leads to the corresponding diastereomeric product. Similarly, the relative energies of transition states that lead to enantiomeric products were employed for the calculation of the enantiomeric excess.

The enthalpy of activation in the gas phase indicates that the *syn* enamine addition to the *si* face of nitrostyrene (i.e., *s-si*) is the most favored mode for **1**–**3**. Whereas the *syn* diastereoselectivities for **2** and **3** are in accordance with the experimental observations, the corresponding enantioselectivities are exactly the opposite. Examination of the relative energies of the transition states $\Delta E_{\text{solvent phase}}$ conveys that transition-state *a-si* (TS(*a-si*)) is in general the most favored mode of addition. This transition state leads to *anti* diastereoselectivity and enantioselectivity toward the 4*S*,5*S* stereoisomer, once again at variance with the experimental observation.[37] Enders and Seki obtained diastereomeric and enantiomeric excess of 88% *de* (*syn*) and 76% *ee* (*S*,*R*), respectively, for the proline-catalyzed Michael addition of **2** to nitrostyrene under methanolic conditions.[4d] Further, the stereoselectivities for the same reaction in solvents such as DMSO, *N*,*N*-dimethylformamide (DMF), and MeCN are reported to be not as good as that obtained in methanol.[4b,d] This observation carries additional significance in the context of the present study, in which we attempt logical improvements to the transition-state models.

It is intriguing to note the lack of consensus between the predicted and observed stereoselectivities. Literature precedence indicates that the stereoselectivity calculated using DFT in proline-mediated reactions generally concurs well with experimental observations.[10b,38] Further, the mutual agreement between the results obtained at the B3LYP and the mPW1PW91 DFT levels in the present study is very good. In an attempt to examine how the trends hold at a higher level of theory, the transition states for the addition of propanal enamine to *trans*-nitropropene were identified at the CBS-4M level. Further, single-point energy calculations for the unassisted pathway was performed by using the B2PLYP/6–31G* level of theory (see the computational methods for further details). These computations were carried out using a model Michael acceptor. Interestingly, the computed stereoselectivities are along similar lines as those selectivities obtained by using the mPW1PW91 and B3LYP levels of theory (see Table S9 in the Supporting Information).

We became interested in probing various factors that could influence the predicted selectivities. One of the reasons behind such a discrepancy could possibly arise from an inadequate transition-state model employed in calculating the stereoselectivities.[39] We envisaged that transition-state stabilization by solvent molecules in the immediate neighborhood could serve as an improvement to the model considered herein. Additionally, the relative energy order between the key transition states obtained in the gas and condensed phases did not remain the same. This disparity implies differential stabilization of the developing charges between different transition states.[40] To examine whether the explicit inclusion of solvent molecule(s) could result in meaningful changes in the reaction energetics, we decided to re-examine the critical selectivity determining C–C bond-formation step with the explicitly included solvent molecule(s).

Solvent-assisted pathways: Although a variety of factors could contribute to the lack of concurrence, as noticed in the preceding sections, one of the leading hints at this juncture came from reports on the critical role played by solvents in Michael addition reactions involving nitrostyrene.[30] In an effort to address the role of protic solvents, such as methanol, on the reaction energetics and to investigate whether the inclusion of explicit solvent molecules would

Table 1. The computed activation parameters[a] at the mPW1PW91 (*M1*) and B3LYP (*M2*) levels of theory for the Michael reaction between proline enamines derived from **1**–**3** with nitrostyrene and the corresponding diastereomeric and enantiomeric excess obtained by using the transition states in the unassisted pathway.

		Mode of approach				*de* [%]	*ee* [%][b]
		a-si	*a-re*	*s-si*	*s-re*		
				$\Delta H^{\neq}$ (gas phase) [kcal mol^{-1}][c]			
1	M*1*	13.2 (2.7)	12.5 (2.0)	10.5 (0.0)	15.5 (4.0)	*syn* (97)	4*R*,5*S* (93)
	M2	17.5 (3.0)	15.9 (1.4)	14.5 (0.0)	19.1 (4.6)	*syn* (98)	4*R*,5*S* (82)
2	M*1*	10.8 (0.7)	12.6 (2.5)	10.1 (0.0)	12.7 (2.6)	*syn* (53)	4*R*,5*S* (97)
	M2	14.9 (0.7)	15.7 (1.5)	14.2 (0.0)	17.0 (2.8)	*syn* (53)	4*R*,5*S* (85)
3	M*1*	12.7 (0.6)	12.9 (0.8)	12.1 (0.0)	14.8 (2.7)	*syn* (46)	4*R*,5*S* (59)
	M2	17.1 (2.0)	16.1 (0.0)	16.3 (0.2)	19.1 (3.0)	*syn* (93)	4*S*,5*R* (16)
				$\Delta G^{\neq}$ (gas phase) [kcal mol^{-1}][c]			
1	M*1*	29.8 (2.0)	28.0 (0.2)	27.8 (0.0)	31.1 (3.3)	*syn* (93)	4*R*,5*S* (17)
	M2	34.3 (2.9)	31.4 (0.0)	31.8 (0.4)	34.8 (3.4)	*syn* (98)	4*S*,5*R* (32)
2	M*1*	27.7 (0.0)	28.1 (0.4)	27.7 (0.0)	29.2 (1.4)	nil	4*R*,5*S* (32)
	M2	31.9 (1.9)	31.3 (0.0)	31.8 (0.5)	33.5 (2.2)	*syn* (82)	4*S*,5*R* (39)
3	M*1*	29.8 (1.8)	28.0 (0.0)	29.3 (1.3)	30.8 (2.8)	*syn* (91)	4*S*,5*R* (80)
	M2	34.2 (2.8)	31.4 (0.0)	33.5 (2.1)	35.0 (3.6)	*syn* (99)	4*S*,5*R* (94)
				$\Delta E^{\neq}$ (solvent phase) [kcal mol^{-1}][d]			
1	M*1*	11.0 (0.0)	11.7 (0.7)	11.6 (0.6)	13.4 (2.4)	*anti* (46)	4*S*,5*S* (96)
	M2	14.2 (0.0)	14.2 (0.0)	14.8 (0.6)	16.1 (1.9)	nil	4*S*,5*S* (92)
2	M*1*	9.2 (0.0)	10.4 (1.2)	12.0 (2.8)	11.4 (2.2)	*anti* (77)	4*S*,5*S* (95)
	M2	10.1 (0.0)	11.9 (1.8)	14.9 (4.8)	14.5 (4.4)	*anti* (65)	4*S*,5*S* (99)
3	M*1*	10.8 (0.0)	12.0 (1.2)	13.7 (2.9)	13.7 (2.9)	*anti* (77)	4*S*,5*S* (99)
	M2	12.9 (0.0)	14.4 (1.5)	16.7 (3.8)	16.7 (3.8)	*anti* (85)	4*S*,5*S* (99)

[a] The activation barriers are with respect to the isolated reactants; the values in parentheses indicate relative barriers with respect to the lowest-energy transition states. [b] See Scheme 2 for numbering of the stereocenters. [c] The activation parameters were obtained at the mPW1PW91/6–311G**//mPW1PW91/6–31G* and B3LYP/6–311G**//B3LYP/6–31G* levels of theory. [d] The activation parameters obtained at the $PCM_{(MeOH)}$/mPW1PW91/6–311G**//mPW1PW91/6–31G* and $PCM_{(MeOH)}$/B3LYP/6–311G**//B3LYP/6–31G* levels of theory.

lead to any changes in the predicted selectivities, a detailed study on the methanol-assisted Michael addition reaction was undertaken.

We recently demonstrated that the inclusion of explicit co-catalysts (or solvents) in transition-state models could bring about dramatic changes in the preferred reaction pathways in the enamine formation between dimethylamine and propanal.[41] Because the addition step in the present situation involves noticeable charge separation, solvent molecules (methanol) in the immediate vicinity of the reaction site can offer effective stabilization of the transition states.[33] Transition-state stabilization through specific solute–solvent interactions is, therefore, considered herein.[42] Two major modes of stabilization were examined, in which the methanol molecule(s) is 1) either coordinated through local hydrogen bonding with the nitro group, represented as L_n hereafter for the convenience of discussion where *n* represents number of methanol molecules participating in transition-state stabilization, or 2) participates in a cyclic cooperative hydrogen-bonding network, represented as C_n, between the acidic proton of the carboxylic acid and the oxygen atoms of the nitro group. Alternatively, a mixed mode in which one methanol molecule maintains a monofunctional coordination whereas another molecule participates in a cooperative interaction was also considered. Such models denoted as L_nC_n can help to maximize the solute–solvent interactions with a given number of surrounding solvent molecules.

First, an elaborate examination of various modes of interaction of methanol molecule(s) with the selectivity determining transition state was carried out on a representative system. The Michael reaction between 3-pentanone enamine and nitrostyrene was chosen for this purpose. All four diastereomeric transition states were identified to estimate the energetic preference toward possible diastereomeric and enantiomeric products. The optimized transition-state geometries for the methanol-assisted pathways, through the L_n and C_n modes, are provided in Figure 3. This approach helped us identify the coordination modes that best agree with the experimental product stereoselectivities. A logical extension of these possibilities is also studied with the inclusion of three explicit methanol molecules. The inclusion of a larger number of solvent molecules should obviously have to bear higher entropic costs and hence we have not considered systems beyond three methanol molecules.

In the L_n mode of stabilization, the methanol molecule(s) participates in a monofunctional interaction with the developing nitroxide ion. This situation is comparable to the unassisted pathway, as the hydrogen bonding between the NO_2 and −COOH groups remains nearly the same. As expected, no major distortion to the transition-state geometry, particularly the reaction coordinate is noticed. In the C_n mode, a cooperative hydrogen-bonding network between the developing nitroxide moiety of nitrostyrene and the carboxylic acid group of proline facilitated by methanol molecule(s) was considered. A detailed examination of different possible transition states in the solvent-assisted model was considered for the reaction between 3-pentanone enamine and nitrostyrene. The insight obtained from this approach has subsequently been extended to other enamines (i.e., **1** and **3**). The protocol is guided by targeting progressively closer stereoselectivity ratios as compared to the experimental values available for 3-pentanone and cyclohexanone.

The computed activation barriers obtained with the solvent-assisted transition-state models through both the L_n and C_n modes are summarized in Table 2. The stabilization offered by the explicitly included methanol molecules is evidently effective in decreasing the activation barriers relative

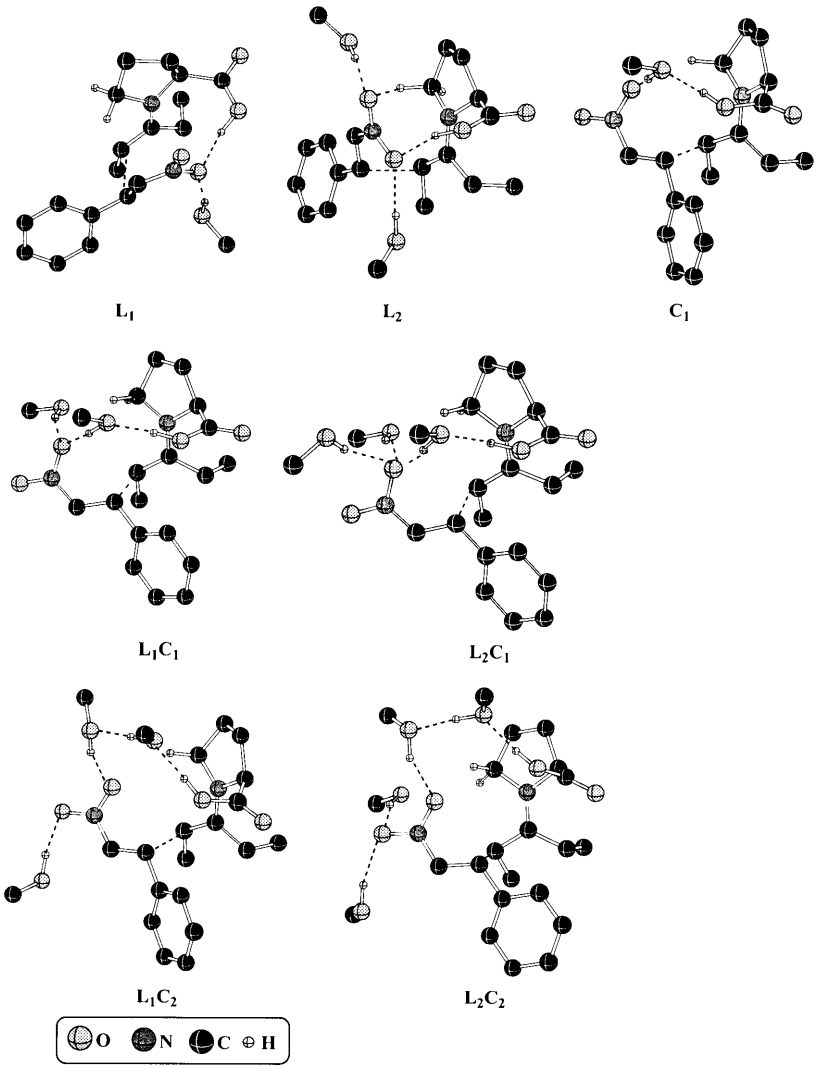

Figure 3. The mPW1PW91/6–31G* optimized transition-state geometries of the *a-re* mode of addition of a proline enamine derived from **2** to nitrostyrene assisted by methanol. The different modes of transition-state stabilizations are depicted as L and C, respectively, for local hydrogen bonding with the nitroxide group and cooperative hydrogen bonding between the carboxylic acid and the nitroxide groups. Only selected hydrogen atoms are shown for clarity.

to the unassisted pathway. The efficiency of all modes of solvent participation, such as L_n, C_n, and L_nC_n, depend on the number of hydrogen-bonding interactions at the transition state. The changes in the relative energies between competitive diastereomeric transition states are of a much higher significance in the present context. The relative activation barriers between the diasteromeric transition states in both the L_1 and L_2 modes exhibited only minor variation relative to the unassisted pathway. For example, the addition of 3-pentanone to nitrostyrene exhibits a preference toward the *a-si* mode of addition in both the L_1 and L_2 modes of stabilization, similar to the unassisted pathway. This prediction implies a product stereochemistry towards the *anti* diastereomer with a preference for the *S*,*S* enantiomer. Because there are no significant changes to the transition-state geometries and the stabilizing weak interactions relative to the unassisted pathway, the predicted stereoselectivity is expected to show similar trends.

In the case of the C_1 model, a preference for the *a-re* mode of addition is noticed (Table 2). This preference leads to *syn* diastereoselectivity with a predicted diastereoisomeric excess of 52% at the $PCM_{(MeOH)}$/mPW1PW91/6–311G**//mPW1PW91/6–31G* level of theory. Although the predicted diasteroselectivity is in agreement with the experimental observation, the enantomeric excess is evidently overestimated (the experimental value is 76% *ee* as opposed to the predicted value of 99% *ee*). The inclusion of additional methanol molecules through the L_1C_1 and L_2C_1 models was then considered. In both these modes, the transition states enjoy further stabilization, but the changes in the predicted stereoselectivities are very marginal in comparison with that obtained through the C_1 model. Hence, at this stage, we started wondering whether further refinement in the predicted selectivity was possible by including both methanol molecules in cooperative interaction, as in the C_2 model. Interestingly, this attempt was indeed fruitful in obtaining improved estimates of the computed selectivity. The predicted diastereoisomeric and enantomeric excess were much closer to the experimental values.[43,44]

The inclusion of additional solvent molecules through mono-coordination modes, such the L_1C_2 and L_2C_2 modes, were not quite effective in improving the predicted enantioselectivities.[45] After having established a reliable model for the solvent-assisted pathway with explicitly included methanol molecules, we turned our attention to the selectivity issues of the C–C bond-forming step for other substrates (i.e., **1** and **3**). In the case of propanal and cyclohexanone, only the C_2 mode of transition-state stabilization was considered in the assisted pathway.

Similar to pentanone (**2**), *syn* diastereoselectivity was predicted for propanal (**1**) and cyclohexanone (**3**) by using the C_2 model in the solvent-assisted pathway (Table 3). The computed values of the diastreo- and enantioselectivities

Table 2. The activation energies[a] at the mPW1PW91 (*M1*) and B3LYP (*M2*) levels of theory for the Michael reaction between proline enamines derived from **2** with nitrostyrene and the corresponding diastereomeric and enantiomeric excess obtained by using different methanol-assisted transition-state models.

Model[a]		Mode of approach				*de* [%]	*ee* [%][c]
		a-si	*a-re*	*s-si*	*s-re*		
		$\Delta E^{\neq}$ (solvent phase) [kcal mol^{-1}][b]					
UA[d]	*M1*	9.2 (0.0)	10.4 (1.2)	12.0 (2.8)	11.4 (2.2)	*anti* (77)	4*S*,5*S* (95)
	M2	10.1(0.0)	11.9 (1.8)	14.9 (4.8)	14.5 (4.2)	*anti* (65)	4*S*,5*S* (99)
L_1	*M1*	4.3 (0.0)	7.3 (3.0)	8.3 (4.0)	6.8 (2.5)	*anti* (97)	4*S*,5*S* (98)
	M2	6.3 (0.0)	9.0 (2.7)	10.3 (4.0)	8.8 (2.5)	*anti* (97)	4*S*,5*S* (99)
L_2	*M1*	2.8 (0.0)	4.4 (1.2)	5.7 (2.5)	3.2 (0.4)	*anti* (77)	4S,5S (32)
	M2	3.2 (0.0)	4.9 (1.7)	9.1 (5.9)	4.3 (1.1)	*anti* (83)	4*S*,5*S* (73)
C_1	*M1*	1.1 (0.7)	0.4 (0.0)	4.4 (4.0)	4.8 (4.4)	*syn* (52)	4*S*,5*R* (99)
	M2	3.0 (0.8)	2.2 (0.0)	6.4 (6.0)	7.1 (6.3)	*syn* (58)	4*S*,5*R* (99)
L_1C_1	*M1*	−1.6 (1.4)	−3.0 (0.0)	0.7 (3.7)	0.7 (3.7)	*syn* (83)	4*S*,5*R* (99)
	M2	−1.0 (0.0)	−1.0 (0.0)	1.2 (2.2)	2.1 (3.1)	nil	4*S*,5*R* (95)
L_2C_1	*M1*	−3.9 (1.0)	−4.9 (0.0)	−2.4 (2.5)	−2.8 (2.1)	*syn* (67)	4*S*,5*R* (97)
	M2	−4.2 (0.9)	−5.1 (0.0)	−2.8 (2.3)	−2.2 (2.7)	*syn* (64)	4*S*,5*R* (96)
C_2	*M1*	−2.6 (1.6)	−4.2 (0.0)	−2.4 (1.8)	−2.9 (1.3)	*syn* (80)	4*S*,5*R* (90)
	M2	−1.7 (0.9)	−2.6 (0.0)	−0.8 (1.8)	−1.1 (1.5)	*syn* (64)	4*S*,5*R* (90)
L_1C_2	*M1*	−6.8 (0.9)	−7.7 (0.0)	−6.1 (1.6)	−6.0 (1.7)	*syn* (64)	4*S*,5*R* (87)
	M2	−6.0 (0.6)	−6.6 (0.0)	−4.5 (2.1)	−4.9 (1.7)	*syn* (47)	4*S*,5*R* (94)
L_2C_2	*M1*	−9.5 (0.0)	−8.6 (0.9)	−7.9 (1.6)	−7.9 (1.6)	*anti* (64)	4*S*,5*S* (87)
	M2	−9.7 (0.0)	−9.0 (0.7)	−8.3 (1.4)	−8.0 (1.7)	*anti* (53)	4*S*,5*S* (88)

[a] The activation barriers are with respect to isolated reactants; the values in parentheses indicate relative barriers with respect to the lowest-energy transition states. [b] The activation parameters were obtained at the $PCM_{(MeOH)}$/mPW1PW91/6–311G**//mPW1PW91/6–31G* and $PCM_{(MeOH)}$/B3LYP/6–311G**//B3LYP/6–31G* levels of theory. [c] See Scheme 2 for numbering of the stereocenters. [d] UA = unassisted pathway.

Table 3. The computed activation parameters[a] at the mPW1PW91 (*M1*) and B3LYP (*M2*) levels of theory for the Michael reaction between proline enamines derived from **1**–**3** with nitrostyrene along with the corresponding diastereomeric and enantiomeric excess obtained by using the transition-state model C_2 in the solvent-assisted pathway.

		Mode of approach				*de* [%]	*ee* [%][b]
		a-si	*a-re*	*s-si*	*s-re*		
		$\Delta H^{\neq}$ (gas phase) [kcal mol^{-1}][c]					
1	M*1*	−10.5 (1.8)	−8.4 (3.9)	−12.3 (0.0)	−10.5 (1.8)	*syn* (89)	4*R*,5*S* (99)
	M2	−7.6 (2.6)	−5.4 (4.9)	−10.3 (0.0)	−8.6 (1.7)	*syn* (89)	4*R*,5*S* (99)
2	M*1*	−11.5 (1.3)	−11.2 (1.6)	−12.8 (0.0)	−12.7 (0.1)	nil	4*R*,5*S* (89)
	M2	−8.6 (1.5)	−8.0 (2.1)	−10.1 (0.0)	−8.9 (1.2)	*syn* (77)	4*R*,5*S* (94)
3	M*1*	−8.3 (2.1)	−6.5 (3.9)	−10.4 (0.0)	−9.3 (1.1)	*syn* (59)	4*R*,5*S* (99)
	M2	−4.6 (3.0)	−3.6 (4.0)	−7.6 (0.0)	−6.5 (1.2)	*syn* (76)	4*R*,5*S* (99)
		$\Delta G^{\neq}$ (gas phase) [kcal mol^{-1}][c]					
1	M*1*	25.9 (1.0)	27.1 (2.2)	24.9 (0.0)	25.2 (0.3)	syn (24)	4*R*,5*S* (97)
	M2	29.3 (1.8)	30.0 (2.5)	27.5 (0.0)	27.5 (0.0)	nil	4*R*,5*S* (97)
2	M*1*	25.3 (0.8)	24.5 (0.0)	25.0 (0.5)	24.5 (0.0)	nil	4*S*,5*R* (40)
	M2	28.6 (1.0)	27.6 (0.0)	28.0 (0.4)	27.6 (0.0)	nil	4*S*,5*R* (32)
3	M*1*	28.8 (2.5)	29.2 (2.9)	26.7 (0.4)	26.3 (0.0)	*anti* (32)	4*R*,5*R* (97)
	M2	32.5 (2.8)	32.0 (2.3)	29.7 (0.0)	29.7 (0.0)	nil	4*R*,5*R* (98)
		$\Delta E^{\neq}$ (solvent phase) [kcal mol^{-1}][d]					
1	M*1*	−1.5 (1.6)	−1.0 (2.1)	−3.1 (0.0)	−2.3 (0.8)	syn (59)	4*R*,5*S* (94)
	M2	−1.0 (0.5)	0.8 (1.7)	−1.5(0.0)	−0.7 (0.8)	*syn* (40)	4*R*,5*S* (89)
2	M*1*	−2.6 (1.6)	−4.2 (0.0)	−2.4 (1.8)	−2.9 (1.3)	*syn* (80)	4*S*,5*R* (90)
	M2	−1.7 (0.9)	−2.6 (0.0)	−0.8 (1.8)	−1.1 (1.5)	*syn* (64)	4*S*,5*R* (90)
3	M*1*	0.5 (1.5)	−1.0 (0.0)	−0.2 (0.8)	0.4 (1.4)	*syn* (82)	4*S*,5*R* (59)
	M2	2.4 (1.5)	0.9 (0.0)	1.5 (0.6)	1.9 (1.0)	*syn* (68)	4*S*,5*R* (46)

[a] The activation barriers are with respect to isolated reactants; the values in parentheses indicate relative barriers with respect to the lowest-energy transition states. [b] See Scheme 2 for numbering of the stereocenters. [c] The activation parameters were obtained at the mPW1PW91/6–311G**//mPW1PW91/6–31G* and B3LYP/6–311G**//B3LYP/6–31G* levels of theory. [d] The activation parameters obtained at the $PCM_{(MeOH)}$/mPW1PW91/6–311G**//mPW1PW91/6–31G* and $PCM_{(MeOH)}$/B3LYP/6–311G**//B3LYP/6–31G* levels of theory.

were in reasonable agreement with the experimental results for **3**. In the case of propanal, correct *syn* selectivity was predicted by using the solvent-assisted pathway.[37] One of the key features that emerges from the present study pertains to the importance of including explicit solvent molecules in transition-state studies in which the simple and direct models fail to reproduce the experimental stereoselectivities. Therefore, it is of particular interest at this juncture to establish the contributing factors that are responsible for the reversal of the selectivities upon considering solvent molecules in close proximity to the reaction site. In the continuum treatment of solvation effects, the specific interactions between the solute and solvent are not considered. Discussion on such interactions observed in the solvent-assisted pathways forms the premise for the next section.

A comparative analysis of the geometries of the transition states in the C_2 model with those of the unassisted pathway for **2** and **3** reveals that the key change is in the C_4-C_3-C_6-C_5 dihedral angle ω around the developing C–C bond. The value of ω also refers to the eclipsing interaction between the phenyl and methyl groups, respectively, on nitrostyrene and the iminium ion around the incipient C–C bond (Figure 4). The maximum change in geometries is noticed for transition states that involve the *anti* enamine (*a-re* and *a-si*). For instance, the eclipsing interaction for the *a-re* mode of addition is $\omega = 58.6°$, whereas the corresponding dihedral angle in the unassisted pathway is $\omega = -56.4°$. Changes in the geometry of the transition states that involve the *anti* enamine can, therefore, modify the weak interactions that are critical to the differential stabi-

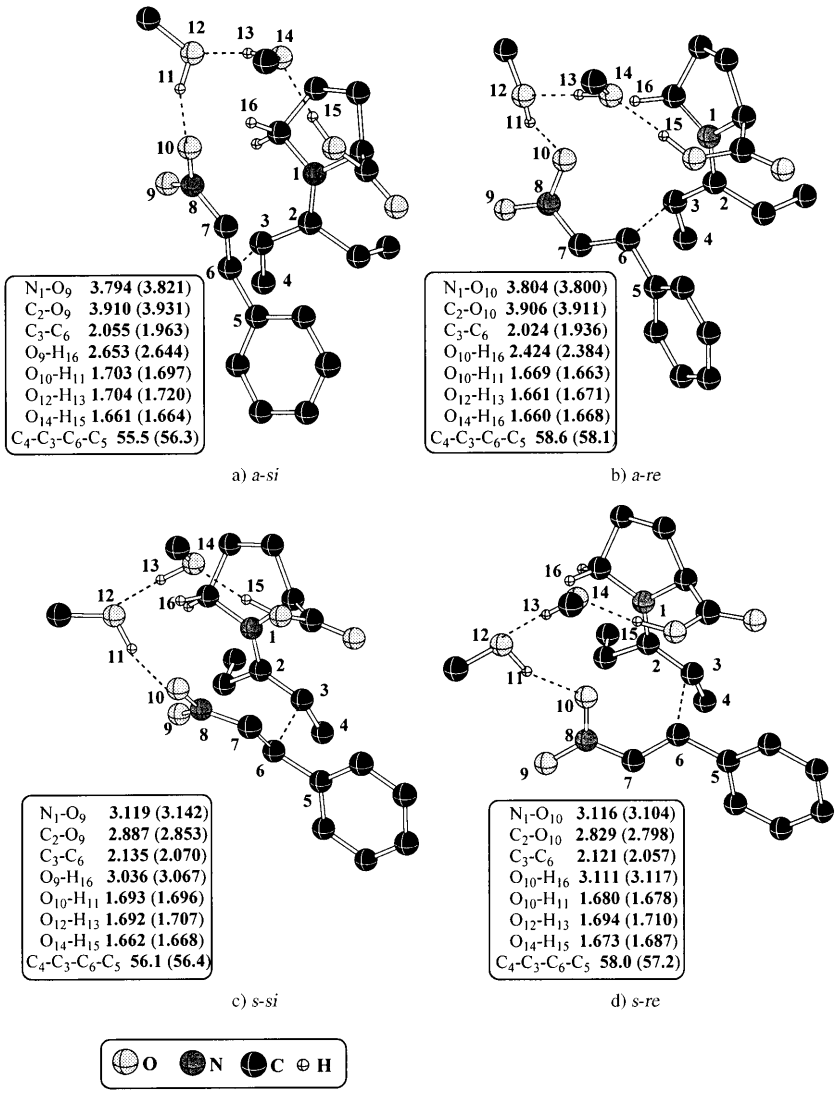

Figure 4. The mPW1PW91/6–31G* optimized transition-state geometries of four stereochemical modes of addition of enamines derived from proline and **2** to nitrostyrene assisted by two methanol molecules in the C_2 model. The values in parentheses refer to the optimized geometric parameters at the B3LYP/6–31G* level of theory. Only selected hydrogen atoms are shown for clarity. Angles are given in degrees and distances in Å.

lization between stereochemically distinct pathways.[46] In the *a-re* transition state, an interesting CH···π stabilization between the phenyl group of nitrostyrene and the alkyl group of the enamine/iminium ion was noticed (i.e., **4b**, Figure 4).[47] Another stabilizing hydrogen-bonding interaction was noticed between the developing nitroxide ion and the skeletal hydrogen atom from the pyrrolidine ring (methylene group; $O_{10}\cdots H_{16}$). It is noteworthy that these stabilizing interactions in similar modes of addition are less effective in the unassisted pathway. In the case of *syn* enamine transition states, the distortions in the solvent-assisted pathway relative to the unassisted pathway are relatively small.

The optimized geometries of the transition states for different modes of addition in the case of cyclohexanone (**3**) exhibited similar structural features to the pentanone system (Figure 5). However, the *syn* enamine additions through the *s-si* and *s-re* modes are more favored than the *anti* enamine additions, namely, *a-si* and *a-re*. Improved hydrogen-bonding interactions in these transition structures could be responsible for the changes in the preferred stereochemical mode of addition in **3**. The interaction between one of the oxygen atoms of the $^{-}NO_2$ group and the pyrrolidine methylene group ($O_{10}\cdots H_{16}$; See **5c** and **5d** in Figure 5) in the *s-si* and *s-re* transition states for the cyclohexanone addition is better (2.7–2.9 Å) than the corresponding interaction in pentanone system (≈3.1 Å). The cumulative effect of such stabilization interactions as discussed presumably results in a low activation barrier for the *s-re* mode of addition in the gas phase ($\Delta G^{\ddagger}$). Although the free energies of activation for **2** and **3** in the gas phase show preference for the *s-re* mode of addition, the difference in the activation barriers for the *s-re* and *s-si* modes of addition is only marginal.

At this juncture, a comparison between the proline-catalyzed Michael addition and aldol reaction will be of interest. The gas-phase calculations that used the DFT studies were generally successful at predicting the correct stereoselectivity in the aldol reactions.[10b] It has been reported that energetically favored transition states for aldol reactions enjoy stabilization through hydrogen-bonding networks and Coulombic interactions. The gas-phase calculations on the Michael reaction, on the other hand, fail to reproduce the experimental stereoselectivities with the range of substrates considered herein. The major difference between these two reactions is the nature of electrophiles, which indeed changes the polarity of the transition state and can lead to differences in kinetic features such as rate and stereoselectivities. In the case of the transition states in the Michael addition, the stabilizing hydrogen-bonding interactions are not as significant as in the aldol reaction.[48] In other words, the extent of intramolecular stabilizations is relatively lower for the transition states in the Michael addition relative to the corresponding proline-catalyzed aldol reactions. Hence, solvents with hydrogen-bonding abilities,

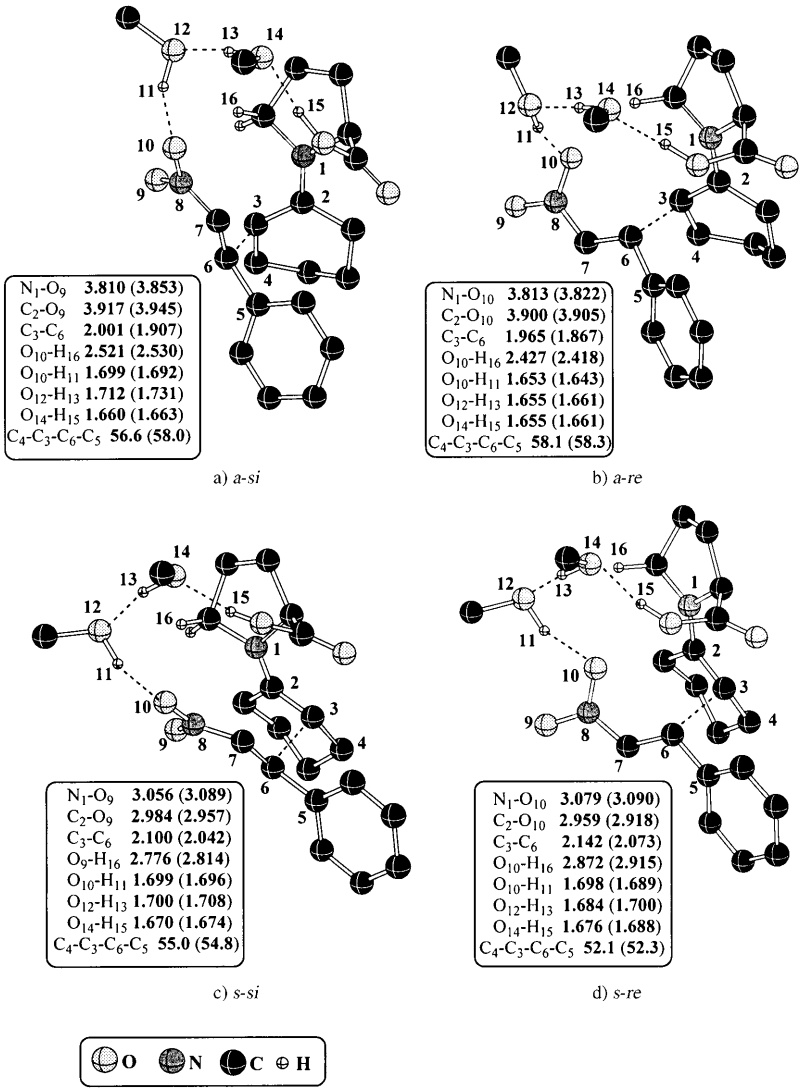

Figure 5. The mPW1PW91/6–31G* optimized transition-state geometries for four stereochemical modes of methanol-assisted addition between the enamine (derived from proline) and **3** to nitrostyrene in the C_2 model. The values in parentheses refer to the optimized bond lengths at the B3LYP/6–31G* level of theory. Only selected hydrogen atoms are shown for clarity. Angles are given in degrees and distances in Å.

such as methanol, could play a vital role in stabilizing the transition states of the Michael addition. An important conjecture is that the higher sensitivity of Michael addition reactions to polar protic solvents could arise from the transition-state stabilization by the solvent molecules as discussed in the previous sections. The factors that could stabilize stereochemically relevant transition states suggest that the specific solute–solvent interactions could be quite critical in the Michael addition. Although the effect of specific hydrogen-bonding interactions of methanol molecules in the transition state is important, it is also necessary to examine the electrostatic effects of the bulk solvent to reliably describe the solvent effect on the energetics of the Michael addition.[49]

The inclusion of a continuum solvent leads to the additional stabilization of transition states with minor changes in the relative activation barriers. The change in the order of relative barriers between the four modes of addition presumably arises from differential electrostatic stabilization offered by the continuum solvation layer. A comparison of the free energies of solvation for various transition states clearly indicates a preference for the *a-re* mode of addition for **2** and **3**.[50] The enantiomeric excess predicted by the $PCM_{(MeOH)}$/mPW1PW91/6–311G**//mPW1PW91/6–31G* level were 90 and 59% *ee* for **2** and **3**, respectively. The diastereomeric excess (about 80% *de*) predicted at the same level of theory for both substrates **2** and **3** was also in close agreement with the observed values (see Scheme 2 for the experimental selectivities). The stereoselectivities computed at the $PCM_{(MeOH)}$/B3LYP/6–311G**//B3LYP/6–31G* level also showed reasonable agreement with the experimental values, although not as impressive as the values obtained at the $PCM_{(MeOH)}$/mPW1PW91/6–311G**//mPW1PW91/6–31G* level of theory.

Transition-state modeling that uses explicit solute–solvent interactions to achieve better estimates of reactivity has been used in several recent studies.[29] Herein, we have established the importance of including explicit solvent molecules along with the bulk solvation effects to gain better insight into the selectivity of a proline-catalyzed Michael reaction.[51] The good agreement between the predicted selectivities from solvent-assisted models with the experimentally observed selectivities supports the proposal that transition-state stabilization through explicit solvent molecules is critical toward improving the right model, in which the direct models are not completely adequate.

Conclusion

We have presented our findings from a detailed investigation on the origins of stereoselectivity in an interesting class of proline-catalyzed Michael reaction by using DFT methods. The commonly used transition-state models in the unas-

sisted pathway (without the inclusion of explicit solvent molecule(s)) failed to reproduce the experimentally observed enantio- and diastereoselectivities in the proline-catalyzed Michael addition of 3-pentanone or cyclohexanone with nitrostyrene. The role of polar protic solvents, such as methanol, was found to be more prominent in improving the selectivity of the Michael reaction. Hence, to address the solvent effect at the atomistic level, transition states were remodeled with the inclusion of explicit solvent molecules. The two different modes of transition-state stabilization involving localized hydrogen bonding (L_n) and cooperative hydrogen bonding (C_n) were examined. Experimentally observed *syn* diastereoselectivity was successfully predicted by using the transition-state model with two explicit methanol molecules in the C_2 mode of stabilization. The prediction was good for widely employed substrates, such as 3-pentanone and cyclohexanone, in an organocatalyzed Michael addition. Careful analysis of intramolecular stabilizing factors, such as Coulombic and hydrogen-bonding interactions, in the transition states was effective in rationalizing the relative trends in the activation barriers between stereochemically different additions of prochiral proline enamines and nitrostyrene. It was found that the participation of explicit methanol molecules at the transition state influences the preferred approach between the enamine and electrophile (nitrostyrene) and can, therefore, modify the pattern of weak interactions. The inclusion of explicit methanol molecules not only helps to stabilize the transition states but also changes the order of preference between four diastereomeric transition states as a result of differential solvation of transition-state structures. In summary, our theoretical studies on the Michael reaction underscore the importance of including explicit and bulk solvation effects in the selectivity-determining transition states toward understanding the stereochemical course of asymmetric reactions.

Computational Methods

All stationary points, such as transition states and minima, were fully optimized in the gas phase at the mPW1PW91/6–31G* and the B3LYP/6–31G* levels of theory[52] by using the Gaussian03 suite of quantum-chemical programs.[53] To evaluate the basis-set effects on the geometries of diastereomeric transition states, additional geometry optimizations using more flexible basis sets were carried out for the unassisted and C_2 models, including 6–31G**, 6-31+G*, and 6-31+G** basis sets. Though the use of B3LYP has recently been questioned for its ability to represent hydrogen-bonding interactions[54] the majority of organic chemistry problems in which the relative activation energies are of prime importance continue to employ the B3LYP functional. Herein, we have also used the mPW1PW91 level of theory along with B3LYP. The choice of modified Perdew–Wang functional for the present investigation was based on the available reports that the mPW1PW91 is good in accounting for likely long-range and hydrogen-bonding interactions.[55] For selected examples, we have compared the results obtained from using these functionals with results from the mPW1K and higher-order composite ab initio methods, such as CBS-4M.

The higher-level calculations were found to be computationally very expensive for relatively larger systems, as in the present study. To examine the general performance of the theoretical methodologies employed herein, a model system was designed by replacing the phenyl group of nitrostyrene with a methyl group. This model system was employed as the Michael acceptor for higher-level calculations in the unassisted pathway. A composite method, such as CBS-4M, is known for improved accuracy.[56] Recent improvements to standard DFT functionals, as proposed by Grimme, incorporate perturbative second-order correlation in a generalized gradient approximation consisting of the Becke exchange; Lee, Yang, and Parr correlation; and Hatree–Fock mixing.[57] The method termed as B2-PLYP was used in conjunction with the 6–31G* basis set for evaluating the single-point energies on the mPW1PW91/6–31G* geometries. The single-point energies were also evaluated at the following levels: 1) mPW1PW91/6–311G**//6–31G*, 2) mPW1PW91/6–311+G**//6–31G*, 3) B3LYP/6–311G**//6–31G*, and 4) B3LYP/6–311+G**//6–31G*. A comparison of single-point energies is provided in Table S9 in the Supporting Information.

The Michael addition of a ketone or an aldehyde to nitrostyrene is expected to involve polarized transition states and hence it is necessary to consider the solvent effect on the reaction. Earlier reports suggest that the reaction rate and product selectivity for this reaction can be improved by using polar protic solvents, such as methanol/isopropanol.[30] The charge stabilization through hydrogen-bonding interactions with explicitly included methanol molecules were studied by identifying the methanol-bound transition states for the nucleophilic addition of enamines derived from ketone/aldehyde to nitrostyrene in the gas phase. The transition-state geometries for the methanol-bound transition structures were arrived at by considering several intuitive initial guess geometries. This approach will enable the inclusion of specific solute–solvent interactions along with bulk solvation effects. The free energies of solvation are more sensitive to the structure and the electron-density distribution. An appropriate theoretical model in conjunction with a quality basis sets should, therefore, be good enough to obtain reasonably accurate estimates of relative solvation energies. Thus, the treatment of both the continuum effects of bulk solvent through an implicit model and the solute–solvent interactions through the explicit consideration of such interactions was included in the present study.

Such an approach in which the explicit solvents are considered together with the implicit model is known as a "cluster-continuum" model. This approach has been in use for quite sometime.[60] One of the major practical issues with this approach is the general difficulty associated with identifying the desired reaction coordinate. Several trial runs are normally required when a new reaction pathway is investigated. These stationary points thus obtained were subsequently subjected to single-point energy calculations by using $PCM_{(MeOH)}$/mPW1PW91/6–311G** and $PCM_{(MeOH)}$/B3LYP/6–311G** methods that use the Tomasi polarized continuum model (PCM) with the united atoms Kohn–Sham (UAKS) radii.[58] The inclusion of diffuse functions in the basis sets were avoided for the PCM single-point energy calculations because this approach could lead to electron-density tails to go beyond the solute cavities generated by the molecularly shaped interlocking spheres. It has also been reported that the use of more extended basis sets often make the results obtained by using continuum models worse.[59] However, to examine the basis-set effect on the trends in the computed activation barriers single-point energies were determined for four diastereomeric transition states in the unassisted and C_2 models at the mPW1PW91 level of theory using the standard basis sets 6–31G*, 6-31+G*, 6–31G**, 6-31+G**, 6–311G**, and 6–311+G** and a non-pople basis set, such as cc-pVDZ. These results are tabulated in Tables S10–S15 in the Supporting Information.

The optimized geometries were characterized as stationary points on the potential-energy surface at respective levels of theory by evaluating the vibrational frequencies. The transition states were characterized by only one imaginary frequency. These frequencies were identified as representing the correct reaction coordinate. The intrinsic reaction coordinate (IRC) calculations were carried out at the mPW1PW91/6–31G* level of theory to further authenticate the transition states.[61] The minimum-energy trajectories are plotted for all the transition states. These plots are provided in Figures S15–S27 in the Supporting Information. Further, we carried out 10% displacement on the transition-state geometry along the direction of the imaginary vibrational frequency and subsequently reopti-

mized the perturbed structure by using the "calcfc" option available in the program. This method was to ensure whether the transition state is genuine and connects to the desired reactants and product. The zero-point vibrational energy corrections (ZPVE) and thermal corrections were applied to the "bottom-of-the-well" values to obtain values for the enthalpy H_{298K} and Gibbs free energy G_{298K} values in the gas phase. In the case of the B3LYP/6–31G* level, a scaled ZPVE (0.9806)[62] was used for estimating enthalpies and free energies. In the condensed phase, the $G_{solvation}$ value obtained using the PCM method (represented as E in the text) is used, which comprises the electronic energy of the polarized solute and electrostatic solute–solvent interaction.[58]

The Wienhold natural bond orbital (NBO) analysis was performed by using NBO3.1 program to compute the natural charges.[63] Topological analysis of the electron densities using the atoms-in-molecule (AIM) approach developed by Bader[64] was carried out by using AIM2000 software.[65] Both NBO and AIM analyses were performed at the mPW1PW91/6–311G**//mPW1PW91/6–31G* level of theory. Most of these data obtained by using the wave functions of important stationary points are employed to support the major points discussed in the text. Further details regarding the NBO and AIM analyses can be found in the Supporting Information.[66,67]

Acknowledgements

Financial support from the Department of Science and Technology, New Delhi (through SR/S1/OC-50/2003) and generous central processing unit time from IIT Bombay Computer Center are gratefully acknowledged. M.P.P. acknowledges CSIR–New Delhi for a Senior Research Fellowship.

[1] a) P. I. Dalko, I. Moison, *Angew. Chem.* **2001**, *113*, 3840; *Angew. Chem. Int. Ed.* **2001**, *40*, 3726; b) B. List, *Tetrahedron* **2002**, *58*, 5573; c) J. Seayad, B. List, *Org. Biomol. Chem.* **2005**, *3*, 719; d) P. I. Dalko, I. Moison, *Angew. Chem.* **2004**, *116*, 5248; *Angew. Chem. Int. Ed.* **2004**, *43*, 5138; e) B. List, *Chem. Commun.* **2006**, 819; f) M. J. Gaunt, C. C. C. Johansson, A. McNally, N. T. Vo, *Drug Discovery Today* **2007**, *12*, 8; g) H. Pellissier, *Tetrahedron* **2007**, *63*, 9267.

[2] a) B. List, R. A. Lerner, C. F. Barbas III, *J. Am. Chem. Soc.* **2000**, *122*, 2395; b) W. Notz, B. List, *J. Am. Chem. Soc.* **2000**, *122*, 7386; c) W. Sakthivel, W. Notz, T. Bui, C. F. Barbas III, *J. Am. Chem. Soc.* **2001**, *123*, 5260; d) A. B. Northrup, D. W. C. MacMillan, *J. Am. Chem. Soc.* **2002**, *124*, 6798; e) A. Bøgevig, N. Kumaragurubaran, K. A. Jørgensen, *Chem. Commun.* **2002**, 620.

[3] a) B. List, *J. Am. Chem. Soc.* **2000**, *122*, 9336; b) B. List, P. Pojarliev, W. T. Biller, H. J. Martin, *J. Am. Chem. Soc.* **2002**, *124*, 827; c) A. Cürdova, W. Notz, G. Zhong, J. M. Betancort, C. F. Barbas III, *J. Am. Chem. Soc.* **2002**, *124*, 1842; d) A. Cürdova, S. Watanabe, F. Tanaka, W. Notz, C. F. Barbas III, *J. Am. Chem. Soc.* **2002**, *124*, 1866; e) W. Notz, F. Tanaka, S. Watanabe, N. S. Chowdari, J. M. Turner, R. Thayumanavan, C. F. Barbas III, *J. Org. Chem.* **2003**, *68*, 9624; f) T. Itoh, M. Yokoya, K. Miyauchi, K. Nagata, A. Ohsawa, *Org. Lett.* **2003**, *5*, 4301; g) Y. Hayashi, W. Tsuboi, I. Ashimine, T. Urushima, M. Shoji, K. Sakai. *Angew. Chem.* **2003**, *115, 3805; Angew. Chem. Int. Ed.* **2003**, 42, 3677; *Angew. Chem. Int. Ed.* **2003**, *42*, 3677; h) Y. Hayashi, W. Tsuboi, M. Shoji, N. Suzuki, *J. Am. Chem. Soc.* **2003**, *125*, 11208; i) A. Cürdova, *Chem. Eur. J.* **2004**, *10*, 1987.

[4] a) S. Hanessian, V. Pham, *Org. Lett.* **2000**, *2*, 2975; b) B. List, P. Pojarliev, H. Martin, *J. Org. Lett.* **2001**, *3*, 2423; c) J. M. Betancort, K. Sakthivel, R. Thayumanavan, C. F. Barbas III, *Tetrahedron Lett.* **2001**, *42*, 4441; d) D. Enders, A. Seki, *Synlett* **2002**, *1*, 26.

[5] T. Bui, C. F. Barbas III, *Tetrahedron Lett.* **2000**, *41*, 6951.

[6] a) B. List, *J. Am. Chem. Soc.* **2002**, *124*, 5656; b) N. Kumaragurubaran, K. Juhl, W. Zhuang, A. Bøgevig, K. A. Jørgensen, *J. Am. Chem. Soc.* **2002**, *124*, 6524; c) A. Bøgevig, K. Juhl, N. Kumaragurubaran, W. Zhuang, K. A. Jørgensen, *Angew. Chem.* **2002**, *114*, 1868; *Angew. Chem. Int. Ed.* **2002**, *41*, 1790; d) N. S. Chowdari, D. B. Ramachary, C. F. Barbas III, *Org. Lett.* **2003**, *5*, 1685.

[7] a) S. P. Brown, M. P. Brochu, C. J. Sinz, D. W. C. MacMillan, *J. Am. Chem. Soc.* **2003**, *125*, 10808; b) G. Zhong, *Angew. Chem.* **2003**, *115*, 4379; *Angew. Chem. Int. Ed.* **2003**, *42*, 4247; c) Y. Hayashi, J. Yamaguchi, K. Hibino, M. Shoji, *Tetrahedron Lett.* **2003**, *44*, 8293; d) Y. Hayashi, J. Yamaguchi, T. Sumiya, M. Shoji, *Angew. Chem.* **2004**, *116*, 1132; *Angew. Chem. Int. Ed.* **2004**, *43*, 1112; e) A. Córdova, H. Sundén, A. Bøgevig, M. Johansson, F. Himo, *Chem. Eur. J.* **2004**, *10*, 3673; f) A. Bøgevig, H. Sundén, A. Córdova, *Angew. Chem.* **2004**, *116*, 1129; *Angew. Chem. Int. Ed.* **2004**, *43*, 1109.

[8] N. Vingola, B. List, *J. Am. Chem. Soc.* **2004**, *126*, 450.

[9] a) S. Bahmanyar, K. N. Houk, *J. Am. Chem. Soc.* **2001**, *123*, 12911; b) S. Bahmanyar, K. N. Houk, *J. Am. Chem. Soc.* **2001**, *123*, 11273; c) F. R. Clemente, K. N. Houk, *Angew. Chem.* **2004**, *116*, 5890; *Angew. Chem. Int. Ed.* **2004**, *43*, 5766; d) C. Allemann, R. Gordillo, F. R. Clemente, P. H.-Y Cheong, K. N. Houk, *Acc. Chem. Res.*, **2004**, *37*, 558; e) F. R. Clemente, K. N. Houk, *J. Am. Chem. Soc.* **2005**, *127*, 11294.

[10] a) L. Hoang, S. Bahmanyar, K. N. Houk, B. List, *J. Am. Chem. Soc.* **2003**, *125*, 16; b) S. Bahmanyar, K. N. Houk, J. Martin, B. List, *J. Am. Chem. Soc.* **2003**, *125*, 2475; c) B. List, L. Hoang, H. Martin, *J. Proc. Nat. Acad. Sci. USA* **2004**, *101*, 5839.

[11] a) B. E. Rossiter, N. M. Swingle, *Chem. Rev.* **1992**, *92*, 771; b) J. d′Angelo, D. Desmaêle, F. Dumas, A. Guingant, *Tetrahedron: Asymmetry* **1992**, *3*, 459; c) M. P. Sibi, S. Manyem, *Tetrahedron* **2000**, *56*, 8033.

[12] a) G. Rosini, R. Ballini, *Synthesis* **1988**, 833; b) R. Tamura, A. Kamimura, N. Ono, *Synthesis* **1991**, 423; c) V. L. Patrocinio, P. R. R. Costa, C. R. D. Correia, *Synthesis* **1994**, 474; d) P. Beak, W. K. Lee, *J. Org. Chem.* **1993**, *58*, 1109; e) T. T. Shawe, A. I. Meyers, *J. Org. Chem.* **1991**, *56*, 2751; f) Y. S. Park, G. A. Weisenburger, P. Beak, *J. Am. Chem. Soc.* **1997**, *119*, 10537; g) R. K. Dieter, C. W. Alexander, L. E. Nice, *Tetrahedron* **2000**, *56*, 2767.

[13] a) A. J. A. Cobb, D. A. Longbottom, D. M. Shaw, S. V. Ley, *Chem. Commun.* **2004**, 1808; b) A. J. A. Cobb, D. M. Shaw, D. A. Longbottom, J. B. Gold, S. V. Ley, *Org. Biomol. Chem.* **2005**, *3*, 84.

[14] a) J. M. Betancort, C. F. Barbas III, *Org. Lett.* **2001**, *3*, 3737; b) A. Alexakis, O. Andrey, *Org. Lett.* **2003**, *5*, 2559; c) O. Andrey, A. Alexakis, G. Bernardinelli, *Org. Lett.* **2003**, *5*, 2559; d) N. Mase, R. Thayumanavan, F. Tanaka, C. F. Barbas III, *Org. Lett.* **2004**, *6*, 2527; e) J. M. Betancort, K. Sakthivel, R. Thayumanavan, F. Tanaka, C. F. Barbas III, *Synthesis* **2004**, 1509; f) O. Andrey, A. Alexakis, A. Tomassini, G. Bernardinelli, *Adv. Synth. Catal.* **2004**, *346*, 1147.

[15] T. Ishii, S. Fujioka, Y. Sekiguchi, H. Kotsuki, *J. Am. Chem. Soc.* **2004**, *126*, 9558.

[16] W. Wang, J. Wang, H. Li, *Angew. Chem.* **2005**, *117*, 1393; *Angew. Chem. Int. Ed.* **2005**, *44*, 1369.

[17] S. Mosse, M. Laars, K. Kriis, A. Kanger, A. Alexakis, *Org. Lett.* **2006**, *8*, 2559.

[18] C. Palomo, S. Vera, A. Mielgo, E. Gomez-Bengoa, *Angew. Chem.* **2006**, *118*, 6130; *Angew. Chem. Int. Ed.* **2006**, *45*, 5984.

[19] a) T. P. Yoon, E. N. Jacobsen, *Angew. Chem.* **2005**, *117*, 470; *Angew. Chem. Int. Ed.* **2005**, *44*, 466; b) T. Okino, Y. Hoashi, T. Furukawa, X. Xu, Y. Takemoto, *J. Am. Chem. Soc.* **2005**, *127*, 119; c) J. Wang, H. Li, X. Yu, L. Zu, W. Wang, *Org. Lett.* **2005**, *7*, 4293; d) A. Berkessel, F. Cleemann, S. Mukherjee, T. N. Muller, J. Lex, *Angew. Chem.* **2005**, *117*, 817; *Angew. Chem. Int. Ed.* **2005**, *44*, 807; e) S. H. McCooey, S. J. Connon, *Angew. Chem.* **2005**, *117*, 6525; *Angew. Chem. Int. Ed.* **2005**, *44*, 6367; f) R. P. Herrera, V. Sgarzani, L. Bernardi, A. Ricci, *Angew. Chem.* **2005**, *117*, 6734; *Angew. Chem. Int. Ed.* **2005**, *44*, 6576; g) M. S. Taylor, E. N. Jacobsen, *Angew. Chem.* **2006**, *118*, 1550; *Angew. Chem. Int. Ed.* **2006**, *45*, 1520.

[20] Y. Hayashi, H. Gotoh, T. Hayashi, M. Shoji, *Angew. Chem.* **2005**, *117*, 4284; *Angew. Chem. Int. Ed.* **2005**, *44*, 4212.

[21] a) T. Mandal, C. Zhao, *Tetrahedron Lett.* **2007**, *48*, 5803; b) L. Gu, G. Zhao, *Adv. Synth. Catal.* **2007**, *349*, 1629.

[22] a) J. Wang, H. Li, B. Lou, L. Zu, H. Guo, W. Wang, *Chem. Eur. J.* **2006**, *12*, 4321; b) A. Hamza, G. Schubert, T. Soós, I. Pápai, *J. Am.*

Chem. Soc. **2006**, *128*, 13151; c) M. Arnó, R. J. Zaragozá, L. R. Domingo, *Tetrahedron: Asymmetry* **2007**, *18*, 157.

[23] Although a comprehensive experimental investigation on the kinetics of the key steps in organocatalyzed reactions is not yet available, the DFT studies by Boyd and co-workers have shown that the enamine formation between proline and acetone has comparable or even higher barriers (in the gas phase) than the ensuing C–C bond-formation step; see K. N. Rankin, J. W. Gauld, R. J. Boyd, *J. Phys. Chem. A* **2002**, *106*, 5155.

[24] a) J.-L. Reymond, Y. Chen, *J. Org. Chem.* **1995**, *60*, 6970; b) J.-L. Reymond, *J. Mol. Catal. B* **1998**, *5-6*, 331.

[25] J. Wang, H. Li, Y. Mei, B. Lou, D. Xu, D. Xie, H. Guo, W. Wang, *J. Org. Chem.* **2005**, *70*, 5678.

[26] a) An alternative view recently proposed by Seebach et al. demonstrates the possibility of oxazolidinone ring formation along with C–C bond formation; see: D. Seebach, A. K. Beck, D. M. Badine, M. Limbach, A. Eschenmoser, A. M. Treasurywala, R. Hobi, W. Prikoszovich, B. Linder, *Helv. Chim. Acta* **2007**, *90*, 425; for related proposals on the involvement of an oxzolidinone–enamine equilibrium in proline-catalyzed reactions, see: b) H. Iwamura, D. H. Well Jr., S. P. Mathew, M. Klussmann, A. Armstrong, D. G. Blackmond, *J. Am. Chem. Soc.* **2004**, *126*, 16312; c) H. Iwamura, S. P. Mathew, D. G. Blackmond, *J. Am. Chem. Soc.* **2004**, *126*, 11770; d) see ref. [10c].

[27] a) P. R. Schreiner, *Chem. Soc. Rev.* **2003**, *32*, 289; b) P. M. Pihko, *Angew. Chem.* **2004**, *116*, 2110; *Angew. Chem. Int. Ed.* **2004**, *43*, 2062; c) G. Dessole, R. P. Herrera, A. Ricci, *Synlett*, **2004**, 2374; d) T. Marcelli, R. N. S. Van Der Haas, J. H. Van Maarseveen, H. Hiemstra, *Angew. Chem.* **2006**, *118*, 943, *Angew. Chem. Int. Ed.* **2006**, *45*, 929; e) J. D. McGilvra, A. K. Unni, K. Modi, V. H. Rawal, *Angew. Chem.* **2006**, *118*, 6276; *Angew. Chem. Int. Ed.* **2006**, *45*, 6130; f) X.-H. Chen, S.-W. Luo, Z. Tang, L.-F. Cun, A.-Q. Mi, Y.-Z. Jiang, L.-Z. Gong, *Chem. Eur. J.* **2007**, *13*, 689.

[28] a) S. Bahmanyar, K. N. Houk, *Org. Lett.* **2003**, *5*, 1249; b) P. H.-Y. Cheong, K. N. Houk, *J. Am. Chem. Soc.* **2004**, *126*, 13912; c) P. H.-Y. Cheong, H. Zhang, R. Thayumanavan, F. Tanaka, K. N. Houk, C. F. Barbas III, *Org. Lett.* **2006**, *8*, 811.

[29] a) S. Kong, J. D. Evanseck, *J. Am. Chem. Soc.* **2000**, *122*, 10418; b) C. Di Valentin, M. Freccero, R. Zanaletti, M. Sarzi-Amadè, *J. Am. Chem. Soc.* **2001**, *123*, 8366; c) J. Chandrasekhar, S. Shariffskul, W. L. Jorgensen, *J. Phys. Chem. B* **2002**, *106*, 8087; d) L. R. Domingo, J. Andrés, *J. Org. Chem.* **2003**, *68*, 8662; e) M. Freccero, C. Di Valentin, M. Sarzi-Amadè, *J. Am. Chem. Soc.* **2003**, *125*, 3544; f) J. I. Mujika, J. M. Mercero, X. Lopez, *J. Am. Chem. Soc.* **2005**, *127*, 4445; g) N. J. Saettel, O. Wiest, *Tetrahedron* **2006**, *62*, 6490; h) R. Gordillo, T. Dudding, C. D. Anderson, K. N. Houk, *Org. Lett.* **2007**, *9*, 501; i) F.-Q. Shi, X. Li, Y. Xia, L. Zhang, Z.-X. Yu, *J. Am. Chem. Soc.* **2007**, *129*, 15503.

[30] It has been reported that methanol or isopropanol serve as good solvents for asymmetric Michael additions catalyzed by proline and its variants; see refs. [1b, 4d, 14a, d].

[31] The *E* enamine, in principle can attack the electrophile either from the *re* or *si* face; hence, eight transition states are identified for the C–C bond-formation step, out of which only four diastereomeric transition states possess a hydrogen-bonding interaction with the –COOH group of the enamine. Besides these transition states, other possible transition states involving the attack of a *Z* enamine on the electrophile also exists; however, the *E* enamine is more stable than the *Z* form by about 4–5 kcal mol^{-1} (both in the gas and solvent phases) at the mPW1PW91/6–31G* level of theory; hence, *E* enamines were considered for further investigation.

[32] Transition states that lack the stabilizing hydrogen-bonding interactions with the carboxylic acid group are 2–5 kcal mol^{-1} higher in energy than those depicted in Scheme 3; see Table S22 in the Supporting Information.

[33] The charges obtained using the natural population analysis at the mPW1PW91/6–311G**//mPW1PW91/6–31G* level of theory revealed that the transition states in the unassisted pathway are quite polar with a substantial charge (−0.5) on each oxygen atom of the developing nitroxide ion; see Figures S3–S5 in the Supporting Information.

[34] C. B. Shinisha, R. B. Sunoj, *Org. Biomol. Chem.* **2007**, *5*, 1287.

[35] See Figure S10 in the Supporting Information for details of the AIM data.

[36] In the case of TS(*a-re*), a better interaction between the developing nitroxide ion and the –COOH group is noticed relative to TS(*s-si*); a less effective stabilization between the developing nitroxide ion and the methylene hydrogen atom from the pyrrolidine ($O_{10}\cdots H_{12}$) is noticed in TS(*s-si*). Other modes of addition possess a relatively higher barrier as they lack of one of these stabilizing interactions in the transition states; for instance, TS(*a-si*) exhibits a less effective Coulombic interaction (between the nitroxide ion and iminium moiety), whereas TS(*s-re*) has a longer hydrogen bond than the lower-energy transition states.

[37] Direct evidence of the proline-catalyzed addition of propanal to nitrostyrene is not available; hence, product stereochemistry is assumed based on the same reaction performed with proline analogues. The addition of aldehydes (3-methylbutanal and pentanal) to nitrostyrene yield a *syn* (*R*,*S*) configuration, unlike the ketone, which results in a *syn* (*S*,*R*) stereochemistry; see refs. [15,16].

[38] Some recent studies: a) L. R. Domingo, M. T. Pitcher, P. Arroyo, *Eur. J. Org. Chem.* **2006**, 2570; b) R. Gordillo, K. N. Houk, *J. Am. Chem. Soc.* **2006**, *128*, 3543; c) S. Bertelsen, M. Marigo, S. Brandes, P. Dinér, K. A. Jørgensen, *J. Am. Chem. Soc.* **2006**, *128*, 12973; d) M. Yamanaka, J. Itoh, K. Fuchibe, T. Akiyama, *J. Am. Chem. Soc.* **2007**, *129*, 6756; e) M. Bruvoll, T. Hansen, E. Uggerud, *J. Phys. Org. Chem.* **2007**, *20*, 206; f) S. Lahiri, S. Yadav, S. Banerjee, M. P. Patil, R. B. Sunoj, *J. Org. Chem.* **2008**, *73*, 435.

[39] a) For details on commonly employed transition-state models for similar reactions; see ref. [10b]; b) it is worth noting that the B3LYP and mPW1PW91 levels are two of the most widely employed functionals in the study of stereoselective reactions; for example, see ref. [38].

[40] a) Four diastereomeric transition states exhibit different solute–solvent interactions when computed with the polarizable continuum model; see Table S18 in the Supporting Information; b) for a similar approach to the evaluation of solute–solvent interaction energies, see: A. G. Martínez, E. T. Vilar, J. O. Barcina, S. de la Moya Cerero, *J. Org. Chem.* **2005**, *70*, 10238.

[41] M. P. Patil, R. B. Sunoj, *J. Org. Chem.* **2007**, *72*, 8202.

[42] The choice of position and orientation of the methanol molecules in these transition states are primarily intuitive; there could be several alternative arrangements of the solvent molecules that can stabilize the developing charges on the nitroxide group. Our approach was to place the solvent molecules so that stronger hydrogen-bonding interactions, such as with the proton from the carboxylic acid group and the nitroxide group, are well maintained in these models.

[43] The effect of basis sets on the computed trends in relative activation barriers were examined at the PCM$_{(methanol)}$/mPW1PW91 level of theory by using a range of Pople and non-Pople type basis sets, such as 6–31G*, 6-31+G*, 6–31G**, 6-31+G**, and cc-pVDZ; the trends in barriers for four diastereomeric transition states in the solvent phase continue to hold well. Although the final conclusion regarding the unassisted and C_2 models did not change with the basis set, the selectivities (*de* and *ee*) were different with respect to differences in the basis sets (see Tables S10 and S15 in the Supporting Information). It was also noticed that the inclusion of diffuse functions on heavy atoms in the solvent-phase single-point calculations resulted in overestimation of enantioselectivity; further, the agreement between the experimental and computed stereoselectivities was poorer upon using the Dunnings basis set (cc-pVDZ).

[44] To verify whether the computed trends in stereoselectivities show variations upon changing the density functional, we performed additional calculations at the mPW1K/6-31+G* level of theory; the mPW1K functional is known to be quite good for obtaining reliable activation barriers in C–C bond-forming reactions (see refs. [44a, b]). Three transition-state models, namely, unassisted, C_1, and C_2, were examined at the mPW1K/6-31+G* level; interestingly,

the C_2 model continued to give the best estimates of stereoselectivity for the Michael addition between the proline enamine derived from 3-pentanone and nitrostyrene (see Tables S16 and S17 in the Supporting Information); a) V. Guner, K. S. Khuong, A. G. Leach, P. S. Lee, M. D. Bartberger, K. N. Houk, *J. Phys. Chem. A* **2003**, *107*, 11445; b) D. Roy, R. B. Sunoj, *Org. Lett.* **2007**, *9*, 4873.

[45] Several alternative arrangements of solvent molecules are likely, especially when they interact in the L_n mode; an exhaustive sampling of the conformational space that encompasses all possible modes of interaction of the solvent through the L_1C_1, L_2C_1, L_1C_2, and L_2C_2 modes is evidently going to be quite laborious when considering that the present study intends to investigate the solvent coordination at the transition states. For these pathways, we considered only a limited number of intuitively guided possibilities. Although all the transition states are fully optimized as a first-order saddle point, similar orientations of the solvent molecules in all four diastereomeric transition states are maintained in the initial guess geometries of the selectivity-determining transition states. The number of coordination possibilities for the cooperative hydrogen-bonding modes, namely C_1 and C_2, are relatively limited as a result of the available space for accommodating solvent molecules capable of participating in hydrogen-bonding interactions between the −COOH group of the enamine and the $-NO_2$ group of nitrostyrene.

[46] In the initial guess geometries for the transition states with cooperative hydrogen bonding (i.e., the C_n or L_nC_n modes), the orientation of nitrostyrene was kept so that multiple methanol molecules could participate in hydrogen-bonding interactions without causing any major distortion to the reaction coordinate, (i.e., the $C_3\cdots C_6$ distance). Further, we tried similar orientations for the unassisted pathways; these additional transition states for the *a-re* mode of addition were higher in energy than the transition state that is discussed for the unassisted route. This group of higher-energy transition states in the unassisted pathway in general exhibited a C_4-C_3-C_6-C_5 dihedral angle of around $\omega = 17°$ (see Table S22 in the Supporting Information for more details).

[47] The CH···π interaction is well documented; selected examples for model systems include a) S. Tsuzuki, K. Honda, T. Uchimaru, M. Mikami, K. Tanabe, *J. Am. Chem. Soc.* **2000**, *122*, 3746; b) S. Tsuzuki, K. Honda, T. Uchimaru, M. Mikami, K. Tanabe, *J. Am. Chem. Soc.* **2002**, *124*, 104; c) the presence of the CH···π interaction in the *a-re* modes of addition is further confirmed by AIM analysis, wherein a bond critical point is identified along the shortest contact between the $-CH_3$ group and the aryl ring (see Figure S13 in the Supporting Information).

[48] Typically, in Michael additions involving nitrostyrene, the O···H distance (in which the oxygen atom is from the NO_2 group) between the electrophile and the hydrogen atom of the pyrrolidine methylene group is 2.4–2.9 Å, whereas the corresponding distance (stabilizing hydrogen-bonding interactions) in the aldol reaction is 2.3–2.4 Å; see refs. [10b,34].

[49] We have adopted a "cluster-continuum" approach to include the effects that might arise from the continuum dielectric medium; see the computational section for more details.

[50] Interestingly, the solute–solvent interaction for the *a-re* mode of addition is invariably higher than the other modes for all three substrates **1**–**3**; see Table S19 in the Supporting Information.

[51] several reports are now available on organocatalytic reactions under aqueous conditions; our studies suggest that the search for proper solvent-assisted transition-state models in such cases is essential to explain the mechanism, stereoselectivity, and related issues.

[52] a) J. P. Perdew, S. H. Chevary, K. A. Vosko, K. A. Jackson, M. R. Pederson, D. J. Singh, C. Fiolhais, *Phys. Rev. B* **1992**, *46*, 6671; b) J. P. Perdew, S. H. Chevary, K. A. Vosko, K. A. Jackson, M. R. Pederson, D. J. Singh, C. Fiolhais, *Phys. Rev. B* **1993**, *48*, 4978; c) J. P. Perdew, K. Burke, Y. Wang, *Phys. Rev. B* **1996**, *54*, 16533; d) C. Adamo, V. Barone, *J. Chem. Phys.* **1998**, *108*, 664; e) A. D. Becke, *J. Chem. Phys.* **1993**, *98*, 5648; f) C. Lee, W. Yang, R. G. Parr, *Phys. Rev. B* **1988**, *37*, 785

[53] M. J. Frisch et al. Gaussian 03 (Revision C.02) Gaussian, Inc., Wallingford CT, **2004**; see the Supporting Information for the full list of citations.

[54] a) H. L. Woodcock. H. F. Schaefer III, P. R. Schreiner, *J. Phys. Chem. A* **2002**, *106*, 11923; b) P. R. Schreiner, A. A. Fokin, R. A. Pascal Jr. , A. de Meijere, *Org. Lett.* **2006**, *8*, 3635; c) J. Zhao, D. G. Truhler, *J. Chem. Theory Comput.* **2007**, *3*, 289; d) M. D. Wodrich, C. Corminboeuf, P. R. Schreiner, A. A. Fokin, P. v. R. Schleyer, *Org. Lett.* **2007** *9*, 1851; e) S. Grimme, M. Steinmetz, M. Korth, *J. Chem. Theory Comput.* **2007**, *3*, 42.

[55] Some select examples of the successful applications of the mPW1PW91 functional: a) A. Pelekh, R. W. Carr, *J. Phys. Chem. A* **2001**, *105*, 4697; b) M. Porembski, J. C. Weisshaar, *J. Phys. Chem. A* **2001**, *105*, 6655; c) R. A. Klein, B. Mennucci, J. Tomasi, *J. Phys. Chem. A* **2004**, *108*, 5851; d) R. A. Klein, M. A. Zottala, *Chem. Phys. Lett.* **2006**, *419*, 254; e) Y. Zhao, D. G. Truhlar, *J. Phys. Chem. A* **2004**, *108*, 6908; f) S. S. Pinto, H. P. Diogo, R. C. Guedes, B. J. C. Cabral, M. E. M. da Piedade, A. M. Simoes, *J. Phys. Chem. A* **2005**, *109*, 9700.

[56] a) J. W. Ochterski, G. A. Petersson, J. A. Montgomery Jr. , *J. Chem. Phys.* **1996**, *104*, 2598; b) J. A. Montgomery Jr. , M. J. Frisch, J. W. Ochterski, G. A. Petersson, *J. Chem. Phys.* **2000**, *112*, 6532.

[57] S. Grimme, *J. Chem. Phys.* **2006**, *124*, 034108.

[58] a) M. Cossi, V. Barone, R. Cammi, J. Tomasi, *Chem. Phys. Lett.* **1996**, *255*, 327; b) E. Cances, B. Mennucci, J. Tomasi, *J. Chem. Phys.* **1997**, *107*, 3032; c) M. Cossi, G. Scalmani, N. Rega, V. Barone, *J. Chem. Phys.* **2002**, *117*, 43.

[59] a) J. B. Foresman, T. A. Keith, K. B. Wiberg, J. Snoonian, M. J. Frisch, *J. Phys. Chem.* **1996**, *100*, 16098; b) Y. Takano, K. N. Houk, *J. Chem. Theory Comput.* **2005**, *1*, 70; c) N. Sadlej-Sosnowska, *Theor. Chem. Acc.* **2007**, *118*, 281.

[60] a) P. Claverie, J. P. Daudey, J. Langlet, B. Pullman, D. Piazzola, M. Duron, *J. Phys. Chem.* **1978**, *82*, 405; b) J. R. Pliego Jr. , J. M. Riveros, *J. Phys. Chem. A* **2001**, *105*, 7241; c) Z. Cao, M. Lin, Q. Zhang, Y. Mo, *J. Phys. Chem. A* **2004**, *108*, 4277; d) B. Balta, G. Monard, M. F. Ruiz-Lopez, M. Antonie, A. Gand, S. Boschi-Muller, G. Branlant, *J. Phys. Chem. A* **2006**, *110*, 7628; e) C. M. Aikens, M. S. Gordon, *J. Am. Chem. Soc.* **2006**, *128*, 12635.

[61] a) C. Gonzalez, H. B. Schlegel, *J. Chem. Phys.* **1989**, *90*, 2154; b) C. Gonzalez, H. B. Schlegel, *J. Phys. Chem.* **1990**, *94*, 5523.

[62] A. P. Scott, L. Radom, *J. Phys. Chem.* **1996**, *100*, 16502.

[63] a) E. D. Glendening, A. E. Reed, J. E. Carpenter, F. Weinhold, NBO Version 3.1; b) A. E. Reed, L. A. Curtiss, F. Weinhold, *Chem. Rev.* **1988**, *88*, 899.

[64] R. F. W. Bader, *Atoms in Molecules: A Quantum Theory*, Clarendon Press, Oxford, **1990.**.

[65] a) AIM2000 (Version 2.0), The Buro fur Innovative Software, SBK-Software, Bielefeld, Germany,; b) F. Biegler-Konig, J. Schonbohm, D. Bayles, *J. Comput. Chem.* **2001**, *22*, 545; c) F. Biegler-Konig, J. Schonbohm, *J. Comput. Chem.* **2002**, *23*, 1489.

[66] See Figures S3–S8 and Figures S9–S14 in the Supporting Information for the NPA charges and AIM analyses, respectively.

[67] The optimized geometries for all the stationary points obtained at different levels of theory, total electronic energies, bond order, natural charges, AIM analyses, and IRC plots for transition states are provided in the Supporting Information.

Received: May 8, 2008
Published online: October 1, 2008

